Monthly Notices
of the
ROYAL ASTRONOMICAL SOCIETY

MNRAS **453,** 1241–1248 (2015) doi:10.1093/mnras/stv1652

λ Bootis stars in the SuperWASP survey

E. Paunzen,[1]★ M. Skarka,[1] P. Walczak,[2,3] D. L. Holdsworth,[4] B. Smalley,[4] R. G. West[5] and J. Janík[1]

[1]*Department of Theoretical Physics and Astrophysics, Masaryk University, Kotlářská 2, CZ-611 37 Brno, Czech Republic*
[2]*Instytut Astronomiczny, Uniwersytet Wrocławski, PL-51-622 Wrocław, Poland*
[3]*Nicolaus Copernicus Astronomical Center, PL-00-716 Warsaw, Poland*
[4]*Astrophysics Group, Keele University, Staffordshire ST5 5BG, UK*
[5]*Department of Physics, University of Warwick, Coventry CV4 7AL, UK*

Accepted 2015 July 20. Received 2015 July 2; in original form 2015 June 1

ABSTRACT

We have analysed around 170 000 individual photometric WASP (Wide Angle Search for Planets) measurements of 15 well-established λ Bootis stars to search for variability. The λ Bootis stars are a small group of late-B to early-F, Pop I, stars that show moderate to extreme (surface) underabundances (up to a factor 100) of most Fe-peak elements, but solar abundances of lighter elements (C, N, O and S). They are excellent laboratories for the study of fundamental astrophysical processes such as diffusion, meridional circulation, stellar winds and accretion in the presence of pulsation. From the 15 targets, 8 are variable and 7 are apparently constant with upper limits between 0.8 and 3.0 mmag. We present a detailed time-series analysis and a comparison with previously published results. From an asteroseismologic study, we conclude that the found chemical peculiarities are most probably restricted to the surface.

Key words: techniques: photometric – stars: chemically peculiar – stars: variables: δ Scuti.

1 INTRODUCTION

The group of λ Bootis stars stand out among the chemically peculiar (CP) stars of the upper main-sequence. The CP stars normally exhibit strong overabundances of elements, probably caused by magnetic fields, slow rotation or atmospheric diffusion (e.g. Netopil et al. 2008). However, the λ Bootis stars are a small group (only 2 per cent) of late-B to early-F stars that show moderate to extreme (surface) underabundances (up to a factor 100) of most Fe-peak elements, but solar abundances of lighter elements (C, N, O and S). Several members of the group exhibit a strong infrared excess and a disc (Paunzen et al. 2003; Booth et al. 2013).

To explain the peculiar chemical abundances, Venn & Lambert (1990) suggested they are caused by selective accretion of circumstellar material. One of the principal features of that hypothesis is that the observed abundance anomalies are restricted to the stellar surface. On the basis of this hypothesis, Kamp & Paunzen (2002) and Martinez-Galarza et al. (2009) developed models which describe the interaction of the star with its local interstellar and/or circumstellar environment, whereby different degrees of underabundance are produced by different amounts of accreted material relative to the photospheric mass. The fact that the fraction of λ Bootis stars on the main sequence is so small would then be a consequence of the low probability of a star–cloud interaction within a limited parameter space. For example, the effects of meridional circulation dissolves any accretion pattern a few million years after the accretion has stopped.

Since the early 1990s, the pulsational behaviour of the group members was extensively studied because almost all λ Bootis stars are located within the classical δ Scuti/γ Doradus instability strip (Paunzen et al. 2002b; Breger et al. 2006; Paunzen & Reegen 2008; Murphy 2014). It was deduced that at least 70 per cent of the group members inside the classical instability strip pulsate. They do so with first and second overtones modes ($Q < 0.020$ d) typical for δ Scuti-type pulsators. Only a few stars, if any, pulsate in the fundamental mode. In general, the amplitudes do not exceed a few mmags. The period–luminosity–colour relation for this group is, within the errors, identical to that of the normal δ Scuti stars (Paunzen et al. 2002b).

In this paper, we have selected 15 targets from the 66 λ Bootis stars in the lists of Gray & Corbally (1998) and Paunzen (2001) which have at least 1000 data points in the Wide Angle Search for Planets (WASP) archive and are fainter than $V = 8$ mag to avoid the effects of saturation. We analysed the time series of these 15 group members to search for variability and compared our result with those in the literature.

Observations, target selection and data analysis are described in Section 2; results are presented and discussed in Section 3. We conclude in Section 4.

★ E-mail: epaunzen@physics.muni.cz

Table 1. Astrophysical parameters of our 15 target stars together with previous published results about their pulsational behaviour. For constant stars, the Amp column gives the upper limit to pulsational amplitudes. A: Paunzen, Heiter & Weiss (1995), B: Paunzen & Handler (1996), C: Paunzen et al. (1998) and D: Paunzen et al. (2002b).

HD	HIP/DM/TYC	V (mag)	$\log T_{\rm eff}$ (dex)	$\sigma_{\log T_{\rm eff}}$ (dex)	$\log L/L_\odot$ (dex)	$\sigma_{\log L/L_\odot}$ (dex)	Const/Var	Δt (h)	Filter	f (d^{-1})	Amp (mmag)	Ref
23392	17462	8.26	3.991	0.012	1.40	0.08	Const	9.5	*b*	–	2.0	C
36726	BD−00 993	8.84	3.978	0.010	1.36	0.07	Const	9.3	*b*	–	3.0	C
83041	47018	8.93	3.852	0.013	1.24	0.07	Var	9.3	*b*	15.16	7.0	B
83277	47155	8.30	3.845	0.012	1.31	0.09	Const	3.5	*b*	–	1.4	D
90821	BD+26 2097	9.47	3.913	0.004	1.60	0.10	Const	2.0	*b*	–	2.2	D
101108	56768	8.88	3.893	0.004	1.29	0.08	Const	24.5	*b*	–	2.0	C
105058	58992	8.90	3.889	0.010	1.40	0.09	Var	1.8	*b*	24.83	3.0	C
120896	67705	8.49	3.861	0.009	1.09	0.08	Var	3.9	*b*	17.79	10.0	D
125889	CD−35 9471	9.85	3.862	0.010	0.91	0.09	–	–	–	–	–	–
184779	CD−44 13449	8.94	3.858	0.010	1.25	0.06	–	–	–	–	–	–
191850	CD−46 13448	9.65	3.869	0.009	1.19	0.07	Var	7.1	*b*	13.53	34.0	A
261904	0750−1747−1	10.21	3.974	0.009	1.48	0.12	Const	4.3	*b*	–	3.5	D
290492	BD−00 980	9.31	3.908	0.008	1.02	0.11	Const	9.2	*b*	–	1.8	D
290799	BD−00 1047	10.70	3.889	0.005	0.83	0.12	Var	7.8	*b*	23.53	6.0	D
294253	BD−03 1154	9.66	4.027	0.007	1.58	0.11	Const	4.7	*V*	–	7.0	C

2 TARGET SELECTION, OBSERVATIONS AND REDUCTIONS

The photometric data used for this study were from SuperWASP; the WASP instruments are described in Pollacco et al. (2006), with the reduction techniques described in Smalley et al. (2011) and Holdsworth et al. (2014). The aperture-extracted photometry from each camera on each night is corrected for primary and secondary extinction, instrumental colour response and system zero-point relative to a network of local secondary standards. The resultant pseudo-V magnitudes are comparable to Tycho V magnitudes.

We have selected all 66 bona fide λ Bootis stars from the lists by Gray & Corbally (1998) and Paunzen (2001) which are fainter than 8th magnitude to avoid effects of saturation of the photometric data. Furthermore, only objects with more than 1000 data points for which no two approximately equal brightness stars within the 3.5-pixel (∼50 arcsec) WASP photometry aperture were processed. In total, we analysed the light curves of 15 group members.

For two stars, HD 101108 and HD 290492, the analysed WASP photometry includes a companion. BD+39 2458B, the companion of HD 101108, is about 7 arcsec away and 2.6 mag fainter, while the companion for HD 290492, TYC 4766-2124-1 (spectral type of G8 III; Paunzen et al. 2002a), is at a distance of about 25 arcsec and $\Delta V = 2.0$ mag.

Employing the methods and starting values listed by Paunzen et al. (2002a,b) we re-evaluated the $\log T_{\rm eff}$ and $\log L/L_\odot$ for our targets. Photometric data were taken from the General Catalogue of Photometric Data (GCPD; Mermilliod, Mermilliod & Hauck 1997).[1] Where possible, averaged and weighted mean values were used throughout. *Hipparcos* parallax measurements (van Leeuwen 2007) for stars with a precision better than 30 per cent were used. Table 1 lists the basic information, the $\log T_{\rm eff}$ and $\log L/L_\odot$ together with results from former pulsation studies.

The light curves were examined in more detail using the PERIOD04 program (Lenz & Breger 2005), which performs a discrete Fourier transformation. The results were checked with those from the CLEANEST and phase-dispersion method computed within the program package PERANSO[2] (Husar 2006). The differences for the different methods are within the derived errors depending on the time-series characteristics, i.e. the distribution of the measurements over time and the photon noise. We applied these methods to the data sets of four pulsating metallic-lined Am stars (Renson 1984, 29800, 37494 and 55094) taken from Smalley et al. (2011). The errors are in the same range as for our target stars lending confidence in the reduction and analysis techniques.

The detailed observational dates and results of the time-series analysis for all targets are listed in Table 2.

3 ANALYSIS

For eight targets, we detected variability (Table 2). Three of them (HD 101108, HD 125889 and HD 184779) are newly discovered pulsators. For seven stars, no statistically significant frequencies were detected. However, we were able to lower the upper limits compared to those previously published. In Fig. 1, the Fourier spectra of HD 83041 (single frequency), HD 125889 (multiperiodic) and HD 294092 (no significant frequency detected) are presented. It is well known that WASP data are affected by daily aliases and systematics at low frequencies (Smalley et al. 2011). The noise at these frequencies (lower than 5 d^{-1}) is certainly not white but, except for HD 83277, we did not detect any suspicious peak below this limit.

Fig. 2 shows the $\log T_{\rm eff}$ versus $\log L/L_\odot$ diagram of our programme stars (Table 1) together with the borders of the δ Scuti and γ Doradus instability strips taken from Breger & Pamyatnykh (1998) and Dupret et al. (2004), respectively. Four stars (HD 23392, HD 36726, HD 261904 and HD 294253) are well outside the instability strips whereas HD 90821 is just on the edge. Variability was not detected for any of these stars, with upper limits between 0.8 and 3.0 mmag. Two apparently constant stars (HD 83277 and HD 290492) are within the instability strips. The case of HD 83277 is discussed below.

[1] http://gcpd.physics.muni.cz/

[2] http://www.peranso.com/

Table 2. Data characteristics, frequencies, amplitudes and upper limits for our targets. The results of the individual stars are described in more detail in Section 3.

HD	HJD(start) (2450000+)	Δt (d)	$N_{\rm data}$	Frequency (d^{-1})	Amplitude (mmag)	Upper limit (mmag)
23392	4721.635 74	859.864 26	14 887			1.0
36726	5496.452 15	478.951 17	5232			1.5
83041	3860.200 96	2204.164 76	11 178	14.5293	1.6	
83277	3860.233 15	749.117 44	5377			3.0[a]
90821	3131.373 78	1094.156 01	4096			0.8
101108	3128.403 56	1108.132 57	4579	26.6100	2.2	
105058	5651.403 81	56.058 100	9137	19.8097	8.9	
				8.9567	4.5	
				9.1293	3.9	
				10.2565	3.5	
				17.7170	3.1	
				20.7920	3.3	
				14.1886	2.2	
				15.9500	2.7	
120896	4516.723 63	1100.875 98	4443	7.6138	5.6	
				19.6300	3.5	
				12.2889	3.0	
				8.4705	2.6	
				9.9511	2.4	
				21.0899	2.3	
				3.0111	2.2	
				20.1347	2.0	
125889	3860.389 89	2246.075 93	28 492	15.6547	3.5	
				5.1457	2.7	
				6.1680	2.1	
184779	3860.440 19	2246.953 36	26 432	12.5687	13.9	
				13.8351	6.8	
				10.4756	3.0	
191850	3860.486 08	2246.914 80	25 537	13.5330	35.1	
				21.0441	8.8	
				23.3159	8.7	
				9.7829	6.6	
				24.8817	6.1	
				12.9278	4.2	
				9.6737	3.1	
				18.8933	3.0	
				36.8489	2.6	
				14.6698	2.0	
261904	5137.626 95	485.731 94	1178			1.8
290492	4743.495 61	1231.907 71	24 418			0.8
290799	5496.479 00	478.924 32	3499	22.5300	7.2	
294253	5496.479 00	478.924 32	3336			1.5

Note. [a]There might be frequencies in the range 1–5 d^{-1} present, see text.

Three stars (HD 83041, HD 120896 and HD 125889) could be, with the errors of $\log T_{\rm eff}$ and $\log L/L_{\odot}$, located in the γ Doradus instability strip. Recently, Paunzen et al. (2014) discovered that the λ Bootis star HD 54272 is also a γ Doradus-type pulsator. For HD 83041 and HD 125889, we were not able to detect any significant frequency in the γ Doradus domain (0.8–5 d^{-1}). However, the lowest frequency (3.0111 d^{-1}) found for HD 120896 could be due to γ Doradus-type pulsation or due to alias effects.

In the following, we discuss the results of some targets in more detail.

HD 83041: Paunzen & Handler (1996) published a frequency of 15.16 d^{-1}. The difference to our result (14.5293 d^{-1}) can be well explained by the very broad peak in their fourier spectrum due to the short time basis of the earlier observations and the resultant spectral window function.

HD 83277: for the range of frequencies higher that 5 d^{-1}, we find no significant amplitudes above 3 mmag. This result is in line with those by Paunzen et al. (2002b). However, the frequency range between 1 and 5 d^{-1} shows a rather rich spectrum which is just at a 4σ level. Follow-up observations are needed to confirm the reality of these frequencies.

HD 101108: this is a multiperiodic pulsator with amplitudes below 2 mmag. We find a rich spectrum of frequencies in the range between 6 and 30 d^{-1}. Due to the low amplitudes, we are not able to identify individual frequencies common in all data sets. This star is a very interesting target for follow-up observations.

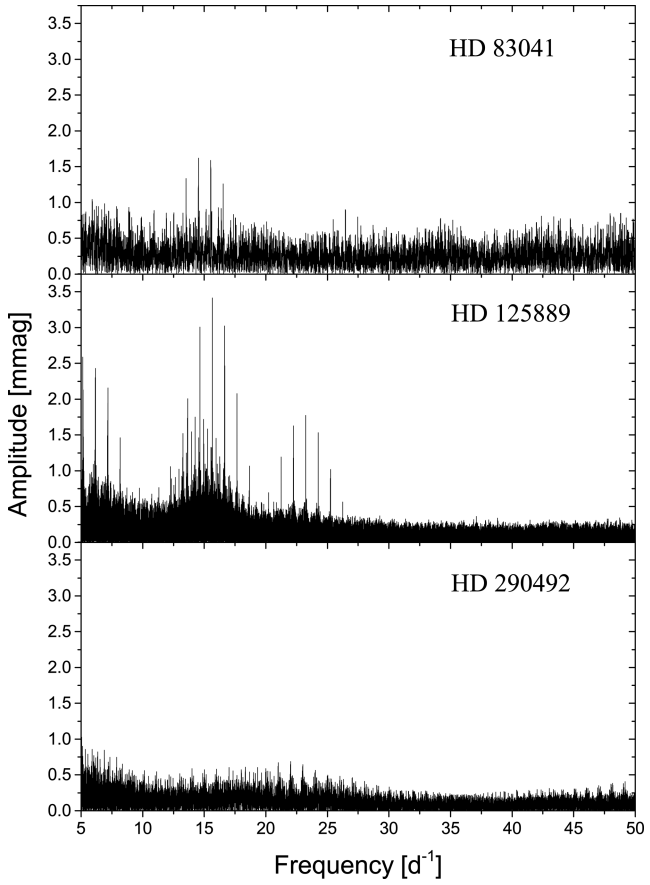

Figure 1. Fourier spectra of HD 83041 (single frequency), HD 125889 (multiperiodic) and HD 294092 (no significant frequency detected).

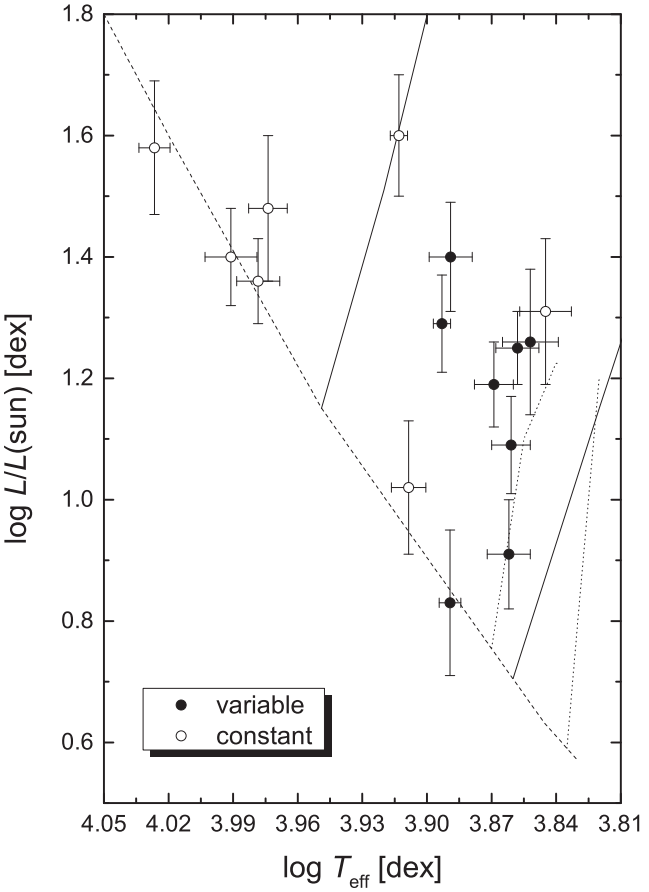

Figure 2. The $\log T_{\rm eff}$ versus $\log L/L_{\odot}$ diagram of our programme stars (Table 1). The borders of the δ Scuti (solid lines) and γ Doradus (dotted lines) instability strips taken from Breger & Pamyatnykh (1998) and Dupret et al. (2004), respectively. The zero-age main sequence (dashed line) is taken from Claret (1995).

HD 105058: our result (19.8097 d^{-1}) is not in line with that (24.8 d^{-1}, about 58 min) published by Paunzen et al. (1998). The latter observed this star for 1.8 h covering less than two pulsation cycles. This fact, together with a possible multiperiodic behaviour, could explain the difference.

HD 290799: the detected frequency is exactly 1 d^{-1} lower than published by Paunzen et al. (2002b). They have observed this object for 7.8 h in Strömgren *b*. There are two WASP data sets from which the second one shows significantly larger amplitudes than the first one. HD 290799 is located in the Orion OB1 association. There are several fainter stars in its vicinity which results in a higher noise level than for the other targets.

3.1 Models for the multiperiodic target stars

The important question we try to answer with our data set is whether or not λ Bootis stars are intrinsically metal-weak (i.e. metal-weak Pop I stars). This does not appear to have been raised very often in the literature. The basic assumption for such an investigation is that all λ Bootis stars are still before the terminal-age main sequence. Casas et al. (2009), for example, made a detailed asteroseismologic analysis of the pulsational behaviour of 29 Cygni (HR 7736, A0.5 Va^{-} λ Boo; Gray 1988). This star is one of the prototypes of the λ Bootis group and exhibits very strong underabundances of the Fe-peak elements compared to the Sun (Paunzen et al. 2002a). From their best-fitting models, they concluded that HR 7736 is an intrinsically metal-weak main-sequence object. We investigated the five multiperiodic target stars HD 105058, HD 120896, HD 125889, HD 184779 and HD 191850 in that respect.

For such an analysis, the accurate knowledge of the basic stellar parameters (effective temperature, surface gravity and metallicity) together with the rotational velocity are needed.

First of all, we explored the $\upsilon \sin i$ values and metallicities ([*M*/H]) of these stars in more detail. In the ESO archive[3] FEROS spectra of these stars, except for HD 105058, with a resolution of about 48 000, covering a spectral range from 3800 to 7900 Å, are available. Initial reductions of the spectra and their conversion into 1D images were carried out within IRAF.[4]

The $\upsilon \sin i$ values were determined measuring the full width at half-maximum (FWHM) of the Mg II 4481 Å line and comparing them with the standard relation listed by Slettebak et al. (1975). We compared the derived FWHM with those of other comparable strong lines and find an excellent agreement. For HD 120896, HD 125889, HD 184779 and HD 191850, we find $\upsilon \sin i$ values of 125, 95, 80 and 60 km s^{-1}, respectively. The errors are about ±5 km s^{-1}.

Synthesized spectra were computed using the program SPECTRUM[5] (Gray & Corbally 1994) and modified versions of the ATLAS9 code

[3] http://archive.eso.org
[4] http://iraf.noao.edu/
[5] http://www.appstate.edu/~grayro/spectrum/spectrum.html

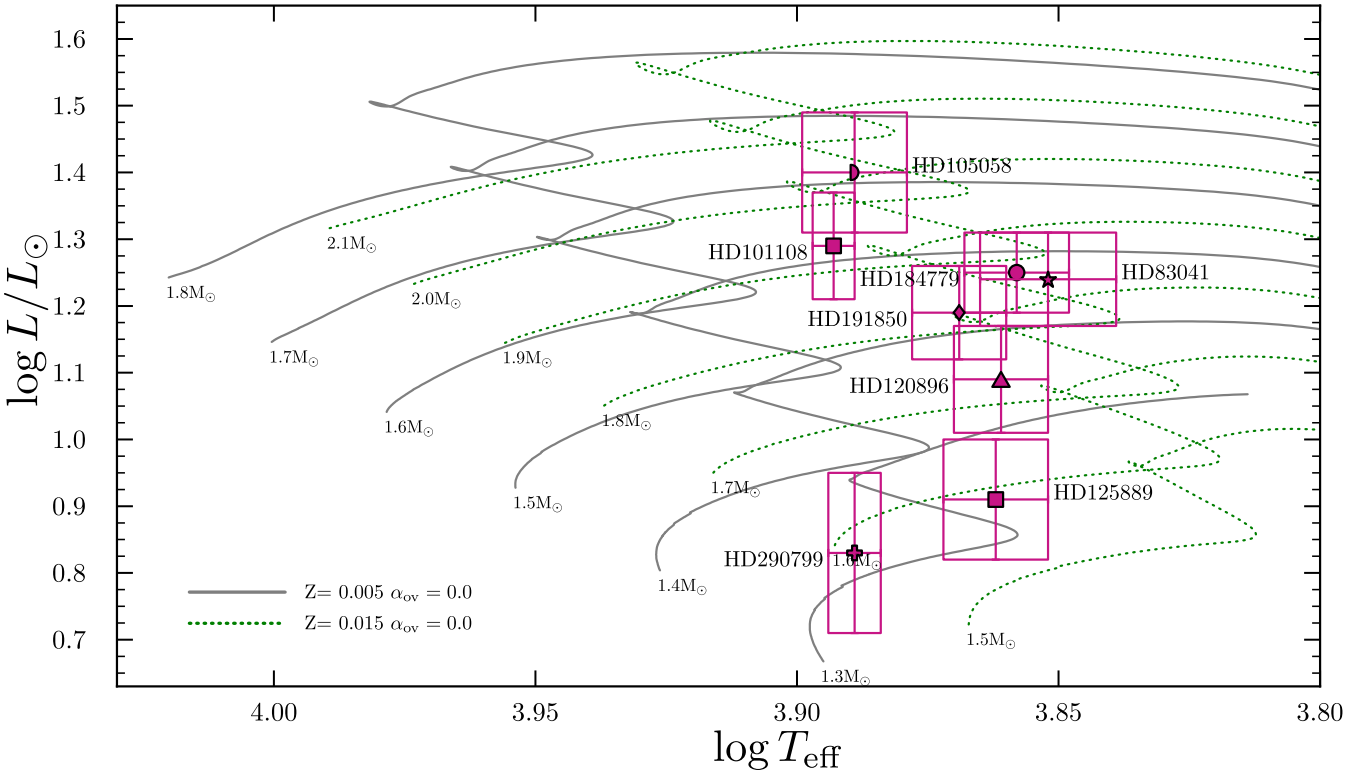

Figure 3. The location of the eight variable stars (Table 2) within the Hertzsprung–Russell diagram. The evolutionary tracks for two different metallicities were calculated as described in Section 3.1. The initial rotational velocity was set to $V_{\rm rot} = 100\,{\rm km\,s^{-1}}$.

taken from the Vienna New Model Grid of Stellar Atmospheres, NEMO[6] (Heiter et al. 2002). The astrophysical parameters were taken from Table 1. The spectra were convolved with the instrumental profile and the rotational profiles using the $\upsilon \sin i$ values listed above. A visual comparison of the observed and synthetic line profiles yields an excellent agreement. To estimate the [*M*/H] value, we used different scaled metallicity models from +0 to −2 dex.

For HD 120896, HD 125889 and HD 184779, we find a very similar metallicity of about −0.5 dex ([*Z*] = 0.004) whereas HD 191850 is more underabundant with [*M*/H] = −0.8 dex ([*Z*] = 0.002). The latter is in perfect accordance with the result of the RAdial Velocity Experiment (RAVE) survey (Siebert et al. 2011).

For HD 105058 the same techniques were applied to the spectrum published by Tomasella, Munari & Zwitter (2010) which has a resolution of only 20 000. The result is $\upsilon \sin i = 135 \pm 5\,{\rm km\,s^{-1}}$ and [*M*/H] = −1.0 dex.

As a next step, theoretical tracks were calculated for several different values of metallicity, 0.004 < [*Z*] < 0.025. We used the Opacity Project data (Seaton 2005), the scaled chemical composition by Asplund et al. (2009), the Warsaw–New Jersey evolutionary code (Pamyatnykh et al. 1998) and the linear non-adiabatic pulsational code by Dziembowski (1977).

3.2 Results from the models

Fig. 3 shows the Hertzsprung–Russell diagram (HRD) with the location of all variable stars. The observational values of the effective temperature and luminosity were taken from Table 1. From this figure we conclude that the stars are on the main sequence only in the case of metallicity [*Z*] > 0.007 for no convective core overshooting, i.e. $\alpha_{\rm ov} = 0.0$. To investigate the influence of the latter, we also calculated evolutionary tracks for two values of the overshooting parameter, namely $\alpha_{\rm ov} = 0$ and 0.2. Fig. 4 shows that the effect is quite strong. A higher efficiency of the core overshooting results in a much more extended main-sequence phase. If we assume $\alpha_{\rm ov} = 0.2$ then [*Z*] > 0.004 is needed for locating the stars on the main sequence. This value is still much higher than deduced from the spectra. From this analysis we would conclude that these objects are intrinsically not metal-weak.

As the next step, we performed a detailed asteroseismic analysis of the detected frequencies in the light of different metallicity values. For this, we used the results of HD 120896, HD 184779 and HD 191850 because they have very similar astrophysical parameters.

Main-sequence hypothesis: to place the stars on the main sequence, we need to assume a metallicity [*Z*] > 0.007 or include effective convective core overshooting. For $\alpha_{\rm ov} = 0.2$ we need about [*Z*] > 0.004. So, if the stars are on the main sequence, we can derived some constrains on the lowest plausible value of the metallicity (Figs 3 and 4).

Fig. 5 shows the instability parameter η, as a function of the frequency for pulsational models. Modes are excited when $\eta > 0$. The models have $\log T_{\rm eff} = 3.862$ and $\log L/{\rm L}_\odot = 1.206$. Different colours indicate various metallicities, circles indicate radial modes ($\ell = 0$) and squares indicate dipole modes ($\ell = 1$). Short vertical lines above the $\eta = 0$ line indicate the observational frequency spectrum for HD 120896 (green), HD 184779 (blue) and HD 191850 (red). We notice that the unstable modes cover almost the entire

[6] http://www.univie.ac.at/nemo

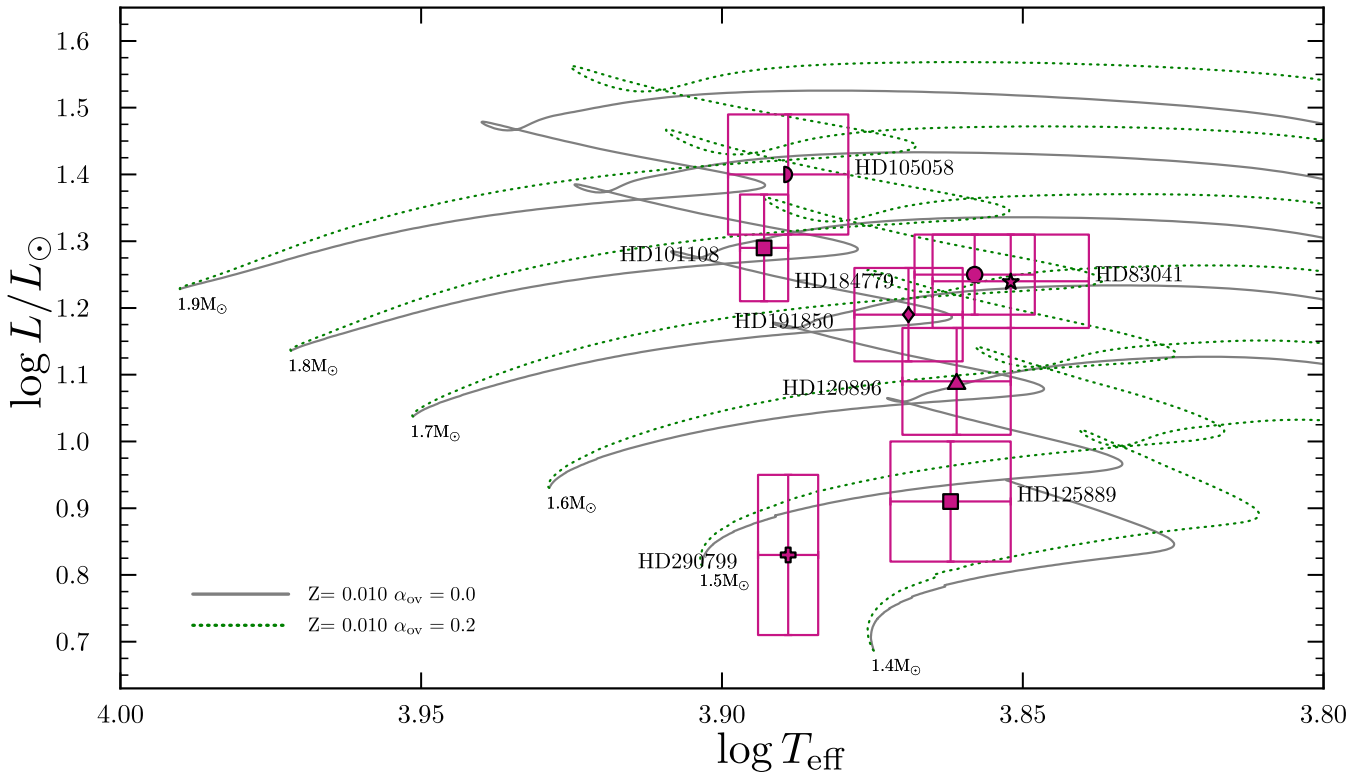

Figure 4. The same as in Fig. 3 but for two values of the overshooting coefficient $\alpha_{ov} = 0.0$ and 0.2, respectively.

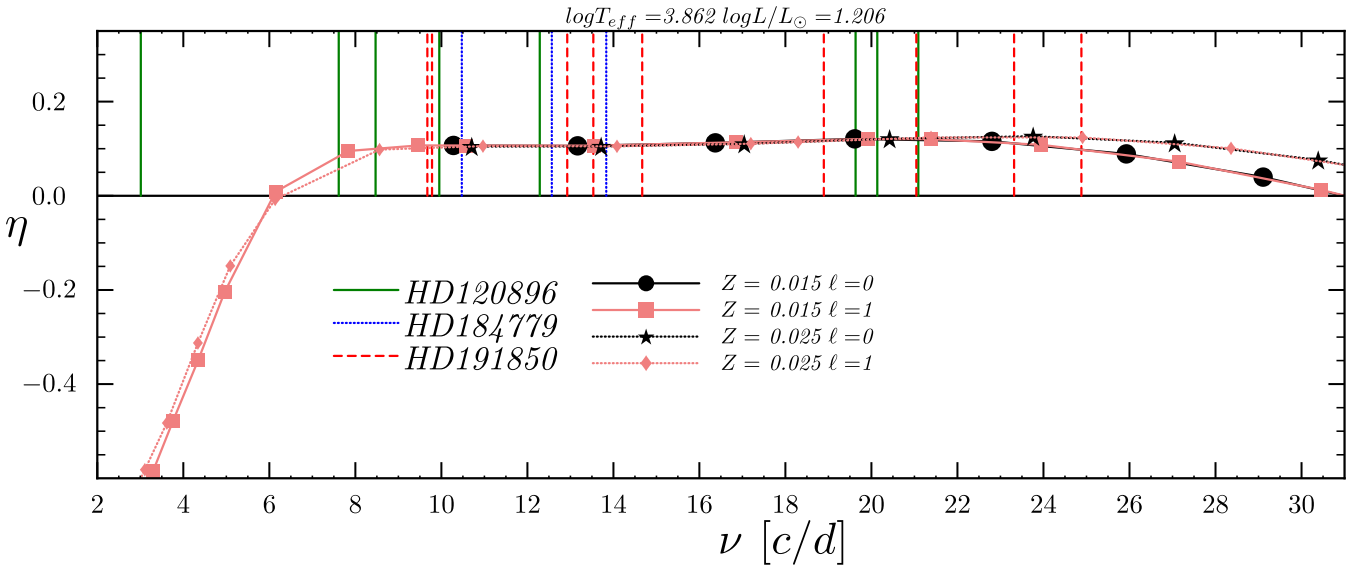

Figure 5. The instability parameter, η, as a function of the pulsational frequency for three star models on the main sequence. All models have $\log T_{eff} = 3.862$ and $\log L/L_\odot = 1.206$. We assumed initial hydrogen abundance $X = 0.7$ and mixing-length parameter $\alpha_{cv} = 1.8$. Different colours indicate various metallicities, circles indicate radial modes ($\ell = 0$) and squares indicate dipole modes ($\ell = 1$). Short vertical lines above the $\eta = 0$ line indicate the observational frequency spectrum for HD 120896 (green), HD 184779 (blue) and HD 191850 (red).

observational spectrum. Increasing the initial hydrogen abundance does not change the results significantly. The same is true if we change the mixing-length parameter to $\alpha_{cv} = 1$. A more significant impact on the models is the overshooting efficiency. For $\alpha_{ov} = 0.2$, we were able to derive models for metallicity $[Z] = 0.005$, while for $\alpha_{ov} = 0.0$, we need $[Z] = 0.008$.

We conclude that if the stars are on the main sequence, a much higher intrinsic metallicity than the values derived from observations are needed to explain the observed frequencies. However, only a detailed mode identification, which is not possible from the presented data, would allow us to define even more strict constrains for the models.

Post-main-sequence hypothesis: in Fig. 6 we present the same analysis as in Fig. 5 but for four different metallicities, $[Z] = 0.004$ (black), 0.007 (green), 0.015 (blue) and 0.025 (red). The left instability border appears at a frequency that is sufficiently low to explain

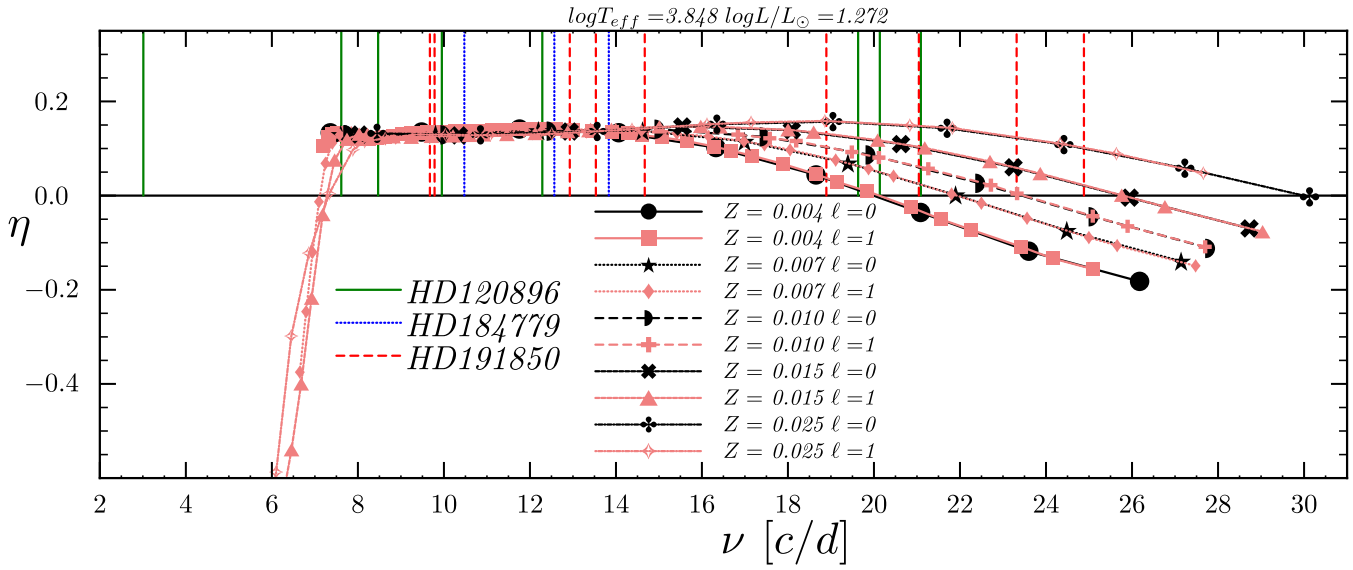

Figure 6. Same as Fig. 5 but for $\log T_{\rm eff} = 3.848$ and $\log L/L_{\odot} = 1.272$.

almost all observed modes. The only exception is a very low frequency of HD 120896. This mode cannot be the retrograde mode shifted to low frequency due to the fast rotation; it would require a rotational velocity of the order of 1000 km s^{-1}. The low-frequency instability border at about $\nu \sim 7$ d^{-1} is almost insensitive to the metallicity, but the high-frequency border depends strongly on [Z]. Because the interaction of convection and pulsation are not well described in the present theory, the true position of the high-frequency instability border is quite uncertain.

A higher value of the initial hydrogen content slightly increases the instability of high-frequency modes. It is due to the fact that high-frequency modes are partially driven through the H I-ionization zone. High-frequency modes have an increase of the work integral near the H I opacity bump. Since convection transports almost the entire energy in this zone, this pulsation driving effect can be artificial. For the chosen effective temperature and luminosity, we were not able to find models beyond the main sequence for [Z] > 0.025. For a more effective core overshooting, we could not find models with [Z] > 0.015. The tracks are shifted to the right on the HRD, and the loop after the main sequence appears for lower values of the effective temperature. The mixing-length parameter, $\alpha_{\rm cv}$, was set to 1.8. The change of this parameter to 1.0 did not cause a significant effect.

In this regime, there are quite strong effects of the chosen $T_{\rm eff}$ and $\log L/L_{\odot}$ values. The instability of modes depends quite strongly on the exact position of a star on the HRD. For a given [Z], a higher effective temperature gives instability for higher frequencies. The low-frequency instability border is shifted to about 9 d^{-1}. For cooler models, we derived instability for lower frequencies, but high-frequency modes were slightly more stable. More luminous models could not explain the instability of high-frequency modes, while less luminous ones have problems with low-frequency modes. This is interesting because the lowest frequencies were found for HD 120896, which is the least luminous star. But its effective temperature is also lower than for the remaining stars, and this effect should cancel the luminosity effect.

The theoretical evolutionary changes of frequencies are of the order of 10^{-7} d^{-1} yr^{-1}, which are too small to detect with the current data.

We conclude that with the frequencies found in this work we are not able to reject the possibility that the stars are beyond the main sequence. Both low and high metallicities are possible because the instability of modes depends mainly on the helium ionization zone.

4 CONCLUSION

We analysed the time series of WASP data sets of 15 well-established λ Bootis stars. This small group of CP objects of the upper main-sequence is an excellent target to investigate the effects of diffusion, rotation and accretion in the presence of classical δ Scuti/γ Doradus-type pulsation.

For eight targets, we were able to detect (multiperiodic) variations with amplitudes between 1.6 and 35.1 mmag. Four of the probable constant stars are not located in the instability strip. A comparison of our results with those from the literature yields an excellent agreement.

We made an asteroseismic analysis of the multiperiodic stars to tackle the question as to whether the chemical peculiarity is intrinsic or restricted to the stellar surface. For this, we estimated the metallicities and projected rotational velocities from high-resolution archival spectra. We then used state-of-the-art pulsation models to characterize the (in)stability properties. From this analysis we conclude that if the stars are still on the main sequence, which is the most accepted hypothesis (Stütz & Paunzen 2006), they are not intrinsically metal-weak. If they are beyond the terminal-age main sequence, the results are ambiguous. We suggest detailed spectroscopic follow-up observations of the presented multiperiodic λ Bootis stars to identify individual modes. Such spectroscopic observations have been already successfully performed for one member of the group, 29 Cygni, by Mkrtichian et al. (2007). Similar studies for δ Scuti stars of comparable magnitudes have been published (Poretti et al. 2009) proving the feasibility. The expected high-precision parallaxes and thus distances as well as luminosities from the *Gaia* satellite mission (Michalik, Lindegren & Hobbs 2015) will hopefully significantly improve the accuracy of the position of the investigated stars in the HRD; at least for those which are not too bright.

ACKNOWLEDGEMENTS

The WASP project is funded and maintained by Queen's University Belfast, the Universities of Keele, St Andrews, Warwick and Leicester, the Open University, the Isaac Newton Group, the Instituto de Astrofisica Canarias, the South African Astronomical Observatory, and by the STFC. This project was supported by the SoMoPro II Programme (3SGA5916), cofinanced by the European Union and the South Moravian Region, the grant GA ČR 7AMB12AT003, LH14300, and the financial contributions of the Austrian Agency for International Cooperation in Education and Research (BG-03/2013 and CZ-09/2014). PW was supported by the Polish National Science Centre grants no. DEC-2013/08/S/ST9/00583. Calculations have been partly carried out using resources provided by Wroclaw Centre for Networking and Supercomputing (http://www.wcss.pl), grant no. 265. We made use of 'The catalog of MK Spectral Types' by B. Skiff. We thank the anonymous referee for the careful reading of our manuscript and the many insightful comments and suggestions. This work reflects our opinion and the European Union is not responsible for any possible application of the information included in the paper.

REFERENCES

Asplund M., Grevesse N., Sauval A. J., Scott P., 2009, ARA&A, 47, 481
Booth M. et al., 2013, MNRAS, 428, 1263
Breger M., Pamyatnykh A. A., 1998, A&A, 332, 958
Breger M., Beck P., Lenz P., Schmitzberger L., Guggenberger E., Shobbrook R. R., 2006, A&A, 455, 673
Casas R., Moya A., Suárez J. C., Martín-Ruíz S., Amado P. J., Rodríguez-López C. Garrido R., 2009, ApJ, 697, 522
Claret A., 1995, A&AS, 109, 441
Dupret M.-A., Grigahcène A., Garrido R., Gabriel M., Scuflaire R., 2004, A&A, 414, L17
Dziembowski W., 1977, Acta Astron., 27, 203
Gray R. O., 1988, AJ, 95, 220
Gray R. O., Corbally C. J., 1994, AJ, 107, 742
Gray R. O., Corbally C. J., 1998, AJ, 116, 2530
Heiter U. et al., 2002, A&A, 392, 619
Holdsworth D. L. et al., 2014, MNRAS, 439, 2078
Husar D., 2006, BAV Rundbrief, 55, 32
Kamp I., Paunzen E., 2002, MNRAS, 335, L45
Lenz P., Breger M., 2005, Commun. Asteroseismol., 146, 53
Martinez-Galarza J. R., Kamp I., Su K. Y. L., Gáspár A., Rieke G., Mamajek E. E., 2009, AJ, 694, 165
Mermilliod J.-C., Mermilliod M., Hauck B., 1997, A&AS, 124, 349
Michalik D., Lindegren L., Hobbs D., 2015, A&A, 574, A115
Mkrtichian D. E. et al., 2007, AJ, 134, 1713
Murphy S. J., 2014, PhD thesis, Univ. of Central Lancashire
Netopil M., Paunzen E., Maitzen H. M., North P., Hubrig S., 2008, A&A, 491, 545
Pamyatnykh A. A., Dziembowski W. A., Handler G., Pikall H., 1998, A&A, 333, 141
Paunzen E., 2001, A&A, 373, 633
Paunzen E., Handler G., 1996, Inf. Bull. Var. Stars, 4301, 1
Paunzen E., Reegen P., 2008, Commun. Asteroseismol., 153, 49
Paunzen E., Heiter U., Weiss W. W., 1995, Inf. Bull. Var. Stars, 4151, 1
Paunzen E. et al., 1998, A&A, 335, 533
Paunzen E., Duffee B., Heiter U., Kuschnig R., Weiss W. W., 2001, A&A, 373, 625
Paunzen E., Iliev I. K., Kamp I., Barzova I. S., 2002a, MNRAS, 336, 1030
Paunzen E. et al., 2002b, A&A, 392, 515
Paunzen E., Kamp I., Weiss W. W., Wiesemeyer H., 2003, A&A, 404, 579
Paunzen E., Skarka M., Holdsworth D. L., Smalley B., West R. G., 2014, MNRAS, 440, 1020
Pollacco D. L. et al., 2006, PASP, 118, 1407
Poretti E. et al., 2009, A&A, 506, 85
Seaton M. J., 2005, MNRAS, 362, 1
Siebert A. et al., 2011, AJ, 141, 187
Slettebak A., Collins G. W., II, Parkinson T. D., Boyce P. B., White N. M., 1975, ApJS, 29, 137
Smalley B. et al., 2011, A&A, 535, A3
Stütz C., Paunzen E., 2006, A&A, 458, L17
Tomasella L., Munari U., Zwitter T., 2010, AJ, 140, 1758
van Leeuwen F., 2007, A&A, 474, 653
Venn K. A., Lambert D. L., 1990, ApJ, 363, 234

This paper has been typeset from a TEX/LATEX file prepared by the author.